Immunity
Article

Plasticity of Leukocytic Exudates in Resolving Acute Inflammation Is Regulated by MicroRNA and Proresolving Mediators

Yongsheng Li,[1] Jesmond Dalli,[1] Nan Chiang,[1] Rebecca M. Baron,[2] Carolina Quintana,[2] and Charles N. Serhan[1,*]
[1]Center for Experimental Therapeutics and Reperfusion Injury, Harvard Institutes of Medicine, Department of Anesthesiology, Perioperative and Pain Medicine, Brigham and Women's Hospital and Harvard Medical School, Boston, MA 02115, USA
[2]Division of Pulmonary and Critical Care Medicine, Department of Medicine, Brigham and Women's Hospital and Harvard Medical School, Boston, MA 02115, USA
*Correspondence: cnserhan@zeus.bwh.harvard.edu
http://dx.doi.org/10.1016/j.immuni.2013.10.011

SUMMARY

The magnitude and duration of acute inflammation are controlled by active resolution programs involving specialized proresolving mediators (SPMs; resolvins and maresins) and microRNAs (miRNAs). Here, we report that miR-466l was temporally regulated in murine exudate-infiltrating leukocytes. Neutrophil miR-466l overexpression in vivo promoted initiation of inflammation that anteceded macrophage expression of this miRNA, which accelerated resolution when overexpressed. In macrophages, miR-466l overexpression increased prostanoids and SPMs (e.g., resolvin D1 [RvD1] and RvD5), which enhanced resolution. RvD1, RvD2, maresin 1 (MaR1), and apoptotic neutrophils reduced miR-466l expression within human macrophages, a feedback regulation that most likely prepares for homeostasis. miR-466l was upregulated in peripheral blood of sepsis patients, and its increase correlated with nonsurvival from sepsis. SPMs and miR-466l regulated transcription factors activator protein 1 and nuclear factor κB1 in miRNA biogenesis. These results demonstrate pivotal roles for SPMs and miR-466l in dynamic leukocyte plasticity during resolution of acute inflammatory responses.

INTRODUCTION

The acute inflammatory response is host protective, and its ideal outcome is timely resolution (Serhan and Savill, 2005). By definition, an exudate contains fluid, cells, and cellular debris from blood vessels deposited in tissues as a result of inflammation, e.g., pus. Several families of lipid mediators (LMs) have been uncovered with the use of self-limited inflammatory leukocyte-rich exudates and a systems approach (Serhan, 2007). These LMs have been coined specialized proresolving mediators (SPMs), which include lipoxins (LXs), resolvins (Rvs), protectins, and maresins (MaRs). These are biosynthesized by inflammatory exudates and possess unique structures with potent anti-inflammatory (e.g., limiting further polymorphonuclear neutrophil [PMN] infiltration) and proresolving (e.g., enhancing macrophage clearance of microbial particles and apoptotic cells) actions, as well as regulate microRNAs (miRNAs) involved in resolution (Recchiuti et al., 2011).

Monocyte and macrophage lineage displays high plasticity and pivotal roles in inflammation (Gordon, 2007; Serhan and Savill, 2005). Upon exposure to stimuli, these cells undergo classical proinflammatory M1 or alternative, anti-inflammatory M2 differentiation (Sica and Mantovani, 2012). A third macrophage subset identified during the resolution phase of self-limited inflammation has been coined resolution-phase macrophages, which display an intermediate phenotype (Bystrom et al., 2008; Russell and Gordon, 2009). Transcriptomic profiling has shown that they are enriched with 15-LOX-1, key in SPM biosynthesis (Stables et al., 2011). We previously reported that SPMs stimulate polarization toward an M2-like profile (Schif-Zuck et al., 2011; Titos et al., 2011), identified miRNAs (i.e., miR-146b, miR-219, miR-208a, and miR-21) critical in resolution, and established RvD1-receptor-dependent resolution circuits (Recchiuti et al., 2011).

These findings led us to question the underlying mechanisms involving SPMs and miRNAs that regulate leukocyte plasticity during resolution of inflammatory exudates. It is now widely appreciated that miRNAs exert actions in the regulation of innate and adaptive immune responses (Sonkoly and Pivarcsi, 2009; Recchiuti et al., 2011). For example, miR-466l contains AU-rich element (ARE) characteristic complementary sequences (AUAAAUA) in the 5′ seed region (Calabrese et al., 2007) and upregulates interleukin-10 (IL-10) in macrophages (Ma et al., 2010), as do SPMs (Recchiuti et al., 2011). Fungal infections with *Saccharomyces cerevisiae* (*S. cerevisiae*) are increased in immune-deficient patients and in patients who have experienced trauma (Kyritsis et al., 2012; McCusker et al., 1994; Underhill et al., 1999). Here, we studied zymosan (Zym) from *S. cerevisiae* and monitored the initiation and resolution phases in both resolving and delayed resolution (Bystrom et al., 2008; Fredman et al., 2012). We report that miR-466l promoted both initiation and resolution of inflammation, as well as macrophage polarization via modulating select ARE-containing targets (ARETs) and LM biosynthesis. Our findings indicate pivotal role(s) for miR-466l-SPM regulatory networks and underscore the dynamic plasticity of leukocytic exudates.

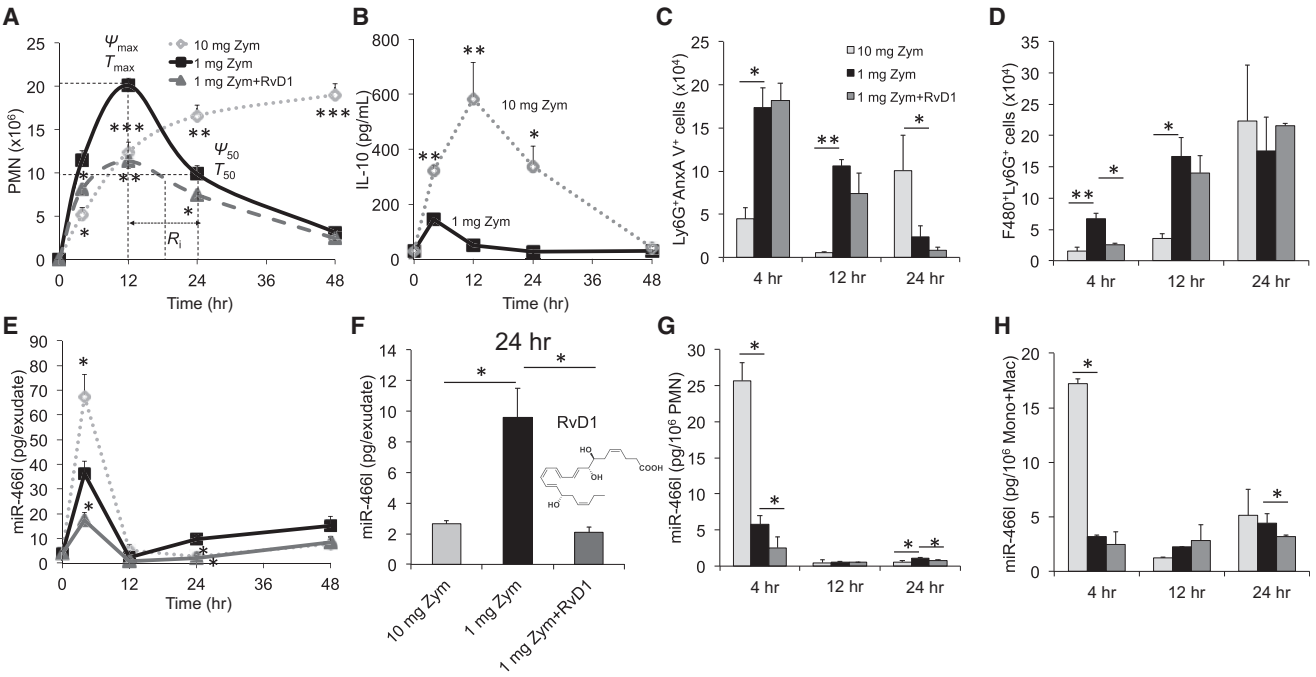

Figure 1. Temporal and Differential Regulation of Exudate Leukocyte miR-466l during Self-limited versus Delayed Inflammation Resolution

Zym was injected (i.p.) for acute peritonitis into male FVB mice divided into three groups: high-dose (10 mg/mouse) challenged, low-dose (1 mg/mouse), and RvD1-treated.

(A) Lavages were collected at indicated intervals, and PMNs were enumerated. See Experimental Procedures and Table S1 for the calculation of resolution indices.

(B) Exudates from 1 and 10 mg of Zym-initiated murine peritonitis (0–48 hr) were collected for IL-10.

(C) Flow cytometry for apoptotic PMNs ($Ly6G^+AnxAV^+$).

(D) Flow cytometry for efferocytosis ($F4/80^+Ly6G^+$).

(E) Total RNAs were isolated at the indicated intervals, and expression of miR-466l was assessed by quantitative PCR (qPCR).

(F) miR-466l expression in each group at 24 hr.

(G and H) Quantitative expression of miR-466l in FACS-sorted PMNs (G), monocytes, and macrophages (H) from murine exudates. Results are expressed as mean ± SEM from at least four independent experiments for each point in each panel. *$p < 0.05$, **$p < 0.01$, and ***$p < 0.001$ versus low-dose group.

See also Figure S1 and Table S1.

RESULTS

miR-466l Is Temporally Regulated during Inflammation Resolution

We sought mechanisms governing SPMs in resolution and tissue homeostasis. To this end, we employed a well-established model of self-limited inflammation for differential comparison with delayed resolution (Bannenberg et al., 2005; Fredman et al., 2012) to address SPM-miR-466l interactions. Zym administered intraperitoneally (i.p.) at 1 mg per mouse elicited a self-limited inflammatory response (Figure 1A). The resolution interval (R_i) was ~12 hr, and the self-resolving challenge was calculated between maximal PMN infiltration and when PMN numbers reduced by ~50% (Figure 1A and Table S1, available online). Monocytes and macrophages increased gradually and at 48 hr were the majority of exudate leukocytes (Figure S1A). For comparison, high dosage led to a continued PMN increase until 48 hr, and at this juncture monocytes and macrophages were ~37%. Excessive PMNs and limited monocyte and macrophage accumulation (Figure 1A and Figure S1A) affirmed that high dosage resulted in delayed resolution and higher cytokines (Figure 1B and Figures S1B–S1D). When RvD1 was given, a significant decrease in PMN infiltration and monocytes was obtained. This regulation of cellular trafficking by RvD1 promoted endogenous proresolving programs that shortened resolution intervals (Figure 1A and Table S1).

The apoptotic PMN number was significantly lower at 4 and 12 hr but higher at 24 hr in the 10 mg Zym group than in the low-dose group (Figure 1C). RvD1 did not significantly affect apoptosis of exudate PMNs. We also monitored macrophages that efferocytosed apoptotic PMNs and found that efferocytosis was lower at 4 and 12 hr in the 10 mg Zym group than in the 1 mg Zym group (Figure 1D). These results indicate that exudate efferocytosis by macrophages (Figure S1E) is higher in self-limited resolution than in delayed resolution.

We monitored miR-466l expression by quantitative real-time PCR by using exogenous *Caenorhabditis elegans* miR-39 (cel-miR-39) to normalize expression between samples as in Mitchell et al., 2008. With a 1 mg Zym challenge, exudate miR-466l markedly increased at 4 hr, most likely representing the PMN content of these exudates, and subsequently decreased sharply at 12 hr (Figure 1E); afterward, it increased

gradually at later intervals (24–48 hr) in the resolution phase. RvD1 reduced miR-466l (Figures 1E and 1F). The amount of miR-466l was ~54% lower at 4 hr but ~183% higher at 24 hr in self-resolving exudates than in delayed-resolving exudates (Figures 1E and 1F). To further address the cellular sources of miR-466l during peritonitis, we employed fluorescence-activated cell sorting (FACS) to isolate exudate PMNs, monocytes, and macrophages for miR-466l assessment. In the 1 mg Zym group, miR-466l was highest in PMNs at 4 hr and then decreased sharply. Subsequently, miR-466l increased slightly at 24 hr (Figure 1G). miR-466l in monocytes and macrophages did not significantly change at either 4 or 12 hr but did show a tendency to increase at 24 hr (Figure 1H). The 10 mg Zym challenge enhanced miR-466l accumulation in PMNs, monocytes, and macrophages at 4 hr while reducing miR-466l in PMNs at 24 hr. Consistent with in vitro results (see below), RvD1 lowered miR-466l in PMNs at 4 and 24 hr, as well as in monocytes and macrophages at 24 hr (Figures 1G and 1H). Together, these results indicate a correlation among PMN apoptosis, clearance of apoptotic cells, and miR-466l, which is temporally and differentially regulated.

miR-466l Regulates Inflammation Resolution

To investigate the actions of miR-466l in inflammation resolution, we performed in vivo transfection in mice and determined the regulation of leukocyte responses by miR-466l with a self-limited challenge. Here, we investigated the dynamic expression of miR-466l in exudate leukocytes and found that miR-466l was upregulated at 4, 24, and 48 hr (Figure 2A). PMN infiltration peaked at ~12 hr in both groups. The maximal PMN number was significantly higher in miR-466l-overexpressing murine peritoneal macrophages than in those transfected with a vector control (VC) (Figure 2B). Although miR-466l overexpression did not shorten R_i, exudate PMNs decreased faster and reached lower amounts at 48 hr (Figures 2B and 2C). To further quantify this, we used the parameter K_{50}, which is the rate of PMN reduction from T_{max} to T_{50}. K_{50} of the miR-466l overexpression group was ~1.2×10^6 cells/hr, ~2.2-fold faster than that of the VCs (Figure 2C). Of note, overexpression of miR-466l in mice did not significantly change the number of apoptotic PMNs in exudates (Figure S2B), whereas it promoted efferocytosis during both the initiation and the resolution phases (Figure 2D). With cell sorting, we found that miR-466l was increased in PMNs at 4 hr and in monocytes and macrophages at 12 and 24 hr in miR-466l-overexpressing exudates (Figures 2E and 2F; overexpression of both miR-466l and GFP was controlled by the same promoter in vivo [see Supplemental Experimental Procedures]). To investigate the role of miR-466l in regulating PMN responses during initiation of self-limited inflammation, we overexpressed miR-466l in murine bone marrow neutrophils (BMNs) and assessed the expression of both proinflammatory and proresolving cytokines (Figures S2E–S2G). Overexpression of miR-466l in BMNs enhanced the expression of interleukin-1β (IL-1β), tumor necrosis factor α (TNF-α), and IL-10 (Figure S2E) and increased chemotaxis to C5a (Figure S2F). Overexpression of miR-466l in BMNs did not significantly stimulate intracellular reactive oxygen species (ROS), whereas it increased TNF-α-stimulated ROS (Figure S2G). To address the impact of neutrophil-associated miR-466l, we performed an adoptive transfer with miR-466l-transfected BMNs and a subsequent challenge (Figure 2H). In these, we found a significantly increased PMN influx at 12 hr, suggesting that miR-466l overexpression gives heightened PMN responses and promotes a proinflammatory PMN phenotype in vivo within the initiation phase.

To address the role of miR-466l in regulating macrophage responses during the initiation phase, we transfected murine peritoneal resident macrophages with either an empty VC or miR-466l ex vivo and carried out adoptive transfer (i.p.) prior to challenge (Figures 2I and 2J and Figures S2H and S2I). In mice that received miR-466l-overexpressing cells, we found a significant reduction in PMNs recruited to the peritoneum in response to challenge. Next, we assessed miR-466l in regulating macrophage responses during the resolution phase. To this end, we performed adoptive transfer of peritoneal macrophages with VC or miR-466l via intraperitoneal injection 12 hr after challenge at the peak of inflammation. After 24 hr, we observed significantly fewer exudate PMNs in mice that received miR-466l-overexpressing macrophages than in mice that received either VC-transfected macrophages or vehicle (Figure 2I); we also obtained significant increases in macrophage efferocytosis at 24 hr (Figure S2I). In addition, injection of macrophages with VC decreased R_i from 12 to 10 hr, and macrophages overexpressing miR-466l further reduced R_i to 8 hr (Figure 2J), indicating that miR-466l expression in macrophages promotes a proresolving phenotype.

miR-466l Upregulates ARETs

Using high-throughput human genome BLAST homology search and quantitative PCR, we identified expression of mature miR-466l in human PMNs, monocytes, and macrophages (Figure S3A-E). To elucidate mechanisms by which miR-466l regulates inflammation resolution, we assessed gene expression profiling by using an inflammation-related genome-wide expression array in human macrophages after miR-466l overexpression or silencing (Figure S3F). Overexpression of miR-466l upregulated several ARET genes, e.g., those encoding IL-26 and IL-1β. In addition, RNA-binding proteins, including cytotoxic granule-associated RNA-binding protein (TIA1) (Asirvatham et al., 2009) and fragile-X-mental-retardation-related protein 1 (FXR1) (Vasudevan and Steitz, 2007; Vasudevan et al., 2007), which are predicted targets for miR-466l (Table S2), were significantly enhanced by miR-466l overexpression and reduced by silencing, whereas mRNAs encoding tristetraprolin (TTP) and human antigen R (HuR) (Asirvatham et al., 2009) were not markedly changed (Figure S3F). Overexpression of miR-466l also elevated KH-type splicing regulatory protein (KSRP) (Briata et al., 2011), an RNA-binding protein without complementary ARE sequences in the miR-466l seed region. Moreover, miR-466l overexpression increased expression of select ARETs, including CD18, FXR1, IL-10, and TNF-α (Figures S3G and S3H).

COX-2, a key enzyme in LM biosynthesis, has complementary AREs in its 3′ UTR (Table S2) and was increased by miR-466l overexpression (Figure S3F). Using luciferase reporters, we found that overexpression of miR-466l in macrophages increased luciferase activity of the COX-2 3′ UTR, but not the COX-1 3′ UTR (Figure S3I). Overexpression of miR-466l enhanced 3′ UTR stability of another ARET, transcriptional factor nuclear factor κB1 (NF-κB1), an action that was lost when the 3′

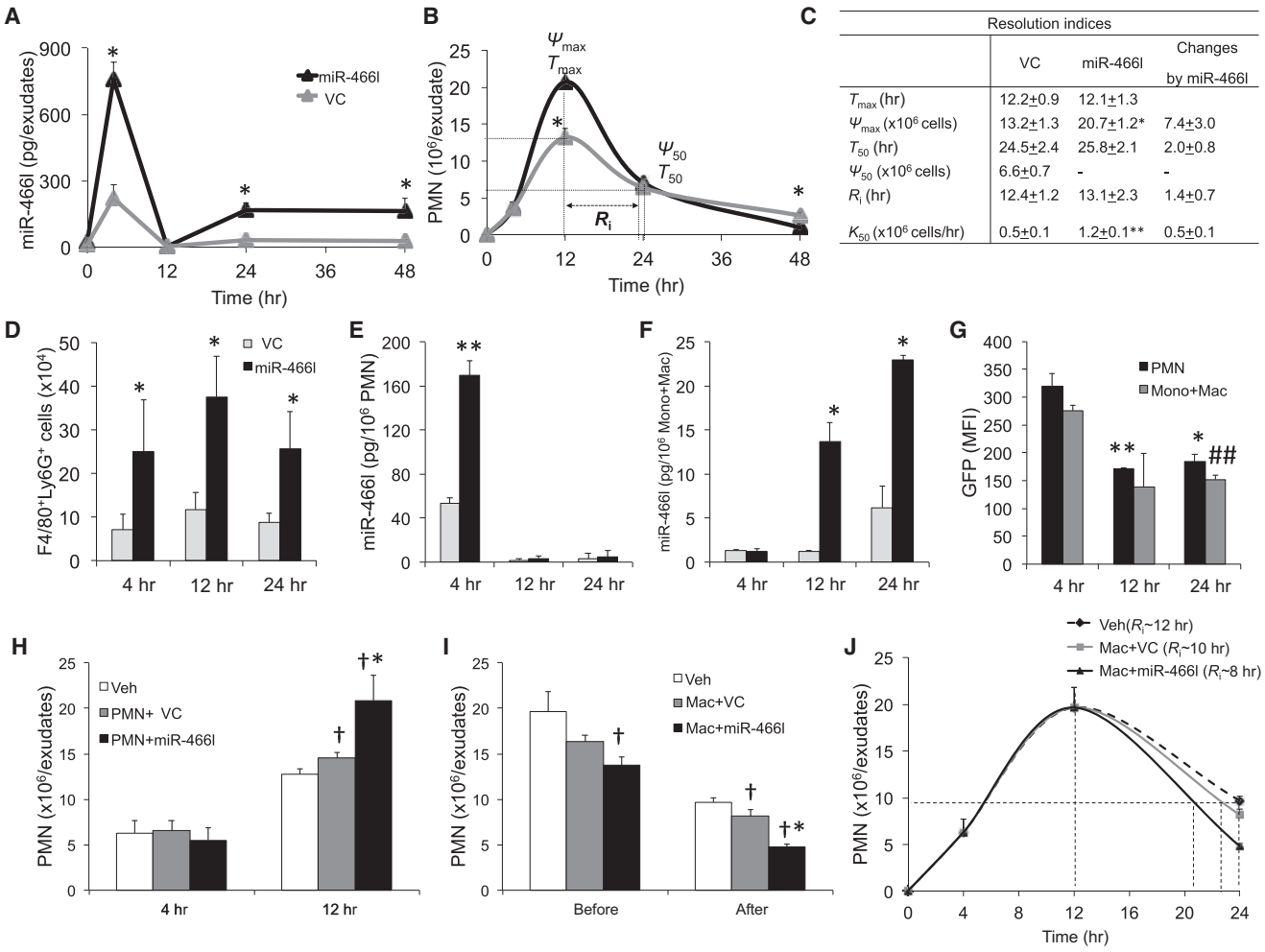

Figure 2. Overexpression of miR-466l in Murine Leukocyte Exudates Regulates Acute Inflammation Resolution

(A–F) Male FVB mice were transfected with VC or miR-466l and then challenged with 1 mg Zym (i.p.) for acute peritonitis. Peritoneal exudates were obtained at the indicated intervals. Results are expressed as mean ± SEM from four independent experiments for each point. *$p < 0.05$ and **$p < 0.01$, miR466l versus VC. (A) miR-466l expression was assessed with qPCR. (B) Infiltrated PMNs were enumerated. (C) Resolution indices for VC and miR-466l groups (see Experimental Procedures). (D) Flow cytometry for efferocytosis ($F4/80^+Ly6G^+$). (E and F) Quantitative expression of miR-466l with FACS-sorted murine exudate PMNs (E) and monocytes and macrophages (Mac) (F).

(G) Expression of GFP with murine exudate PMNs, monocytes, and macrophages from miR-466l-overexpressing mice. Results are expressed in median fluorescence intensities (MFIs) as mean ± SEM from three independent experiments for each point. *$p < 0.05$, PMNs at 4 versus 24 hr; **$p < 0.01$, PMNs at 4 versus 12 hr; ##$p < 0.01$, monocytes and macrophages at 4 versus 24 hr.

(H) VC- and miR-466l-transfected murine BMNs (3×10^6/mouse) were injected into murine tail vein 5 min prior to intraperitoneal challenge with 1 mg Zym. Peritoneal PMN numbers were counted at 4 or 12 hr. Results are expressed as mean ± SEM from at least three independent experiments for each point. †$p < 0.05$, versus vehicle (Veh; saline); *$p < 0.05$, versus VC.

(I) VC or miR-466l murine peritoneal macrophages (7.5×10^4/mouse) were transferred i.p. into mice 5 min prior to or 12 hr after intraperitoneal challenge with 1 mg Zym. Peritoneal PMNs were counted at 12 hr (before challenge) or 24 hr (after challenge). Results are expressed as mean ± SEM from at least three independent experiments for each point. †$p < 0.05$, versus Veh (saline); *$p < 0.05$, versus VC.

(J) Mice were injected i.p. with Veh (saline), VC, or miR-466l-overexpressing macrophages (7.5×10^4/mouse) 12 hr after Zym intraperitoneal challenge for calculation of resolution intervals. Results are expressed as mean ± SEM from at least three independent experiments for each point.

See also Figure S2.

UTR was mutated (Figure S3I and Table S2), indicating that miR-466l upregulates ARETs by stabilizing the 3′ UTR of targets.

miR-466l Mediates Resolution-Phase Macrophage Polarization

We next questioned whether miR-466l also regulates macrophage plasticity. Using multicolor immunofluorescence staining and flow cytometry, we found that markers associated with M1 macrophages—iNOS (1,064 ± 47 versus 389 ± 11 median fluorescence intensity [MFI]), COX-2 (1,695 ± 169 versus 1,339 ± 290 MFI), and CD11c (1,066 ± 44 versus 787 ± 78 MFI)—were upregulated in human macrophages overexpressing miR-466l (Figure 3A and Figure S3F). miR-466l overexpression also upregulated expression of M2 macrophage markers—CD206

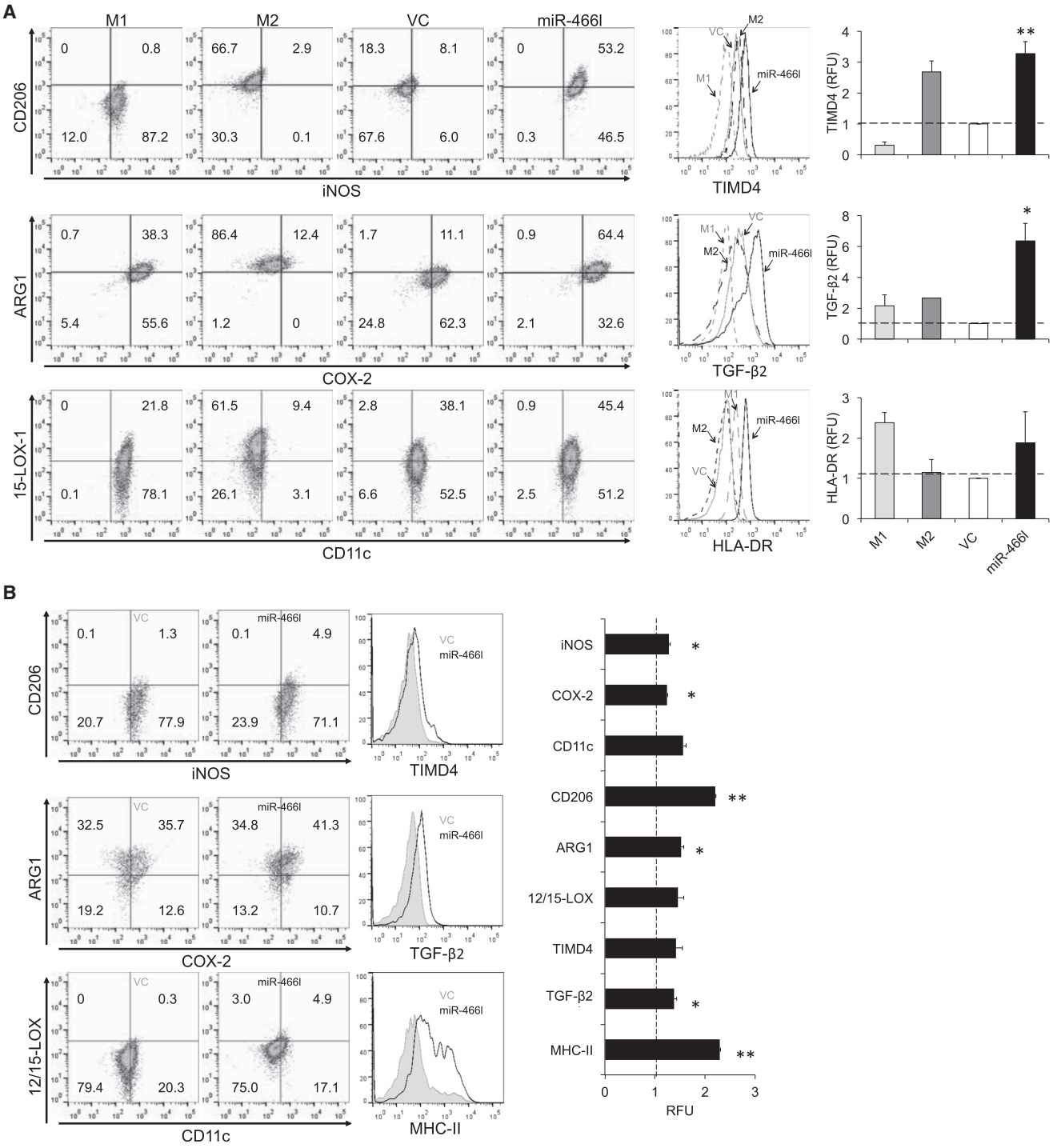

Figure 3. miR-466l Mediates Resolution-Phase Macrophage Polarization

(A) M1 and M2 macrophages were obtained from human peripheral-blood mononuclear cells. VC and miR-466l were transfected into human macrophages for 72 hr (37°C). Phenotypes were assessed by flow cytometry after multicolor staining with fluorescent-conjugated antibodies. Relative fluorescence units (RFU) are normalized against VC and expressed as mean ± SEM from four independent experiments. *$p < 0.05$ and **$p < 0.01$, miR-466l versus VC.

(B) FVB mice were transfected with VC or miR-466l (48 hr) and then challenged with 1 mg Zym for 48 hr. Lavage peritoneal cells stained with three fluorescent-conjugated antibodies were analyzed by flow cytometry analysis. Representative flow cytometry histograms are shown. RFU are normalized against VC and expressed as mean ± SEM from four independent experiments. *$p < 0.05$ and **$p < 0.01$, versus VC.

See also Figure S3 and Table S2.

(1,146 ± 129 versus 216 ± 33 MFI), ARG1 (1,420 ± 171 versus 1,027 ± 5 MFI), and 15-LOX-1 (1,173 ± 80 versus 790 ± 10 MFI)—as well as the resolution-phase macrophage markers TIMD4 (2,612 ± 317 versus 797 ± 1 MFI), HLA-DR (26 ± 11 versus 21 ± 8 MFI), and TGFβ2 (1,163 ± 45 versus 288 ± 36 MFI). These results are consistent with those obtained with murine peritoneal monocytes and macrophages at 48 hr (Figure 3B) and together indicate that miR-466l mediates polarization to a resolution-phase macrophage phenotype (Stables et al., 2011) with characteristics of both classic M1 and M2 lineages.

miR-466l Regulates LM Biosynthesis

Using LM metabololipidomics, we identified and profiled SPMs, including LXA_4, RvD1, and RvD5, as well as proinflammatory LMs (Figures 4). LM amounts were determined by multiple-reaction monitoring, where overexpression of miR-466l in human macrophages gave elevated prostaglandins (PGs) (PGE_2 > PGD_2 > $PGF_{2\alpha}$) and SPMs (RvD2 > RvD5 > RvD1) (Figure 4D and Table S3A). In exudates, overexpression of miR-466l led to a significant upregulation of COX products (PGE_2 > PGD_2 > $PGF_{2\alpha}$) and SPMs (RvD1 > PD1 > RvD5 > MaR1) (Table S3B). LTB_4 was not increased by miR-466l in either human macrophages or peritonitis exudates (Figure 4D, Table S3). Hence, miR-466l facilitates PG and SPM biosynthesis during acute inflammation resolution.

miR-466l Enhances Macrophage Chemotaxis and Phagocytosis by Increasing SPM Production

Given that successful clearance of pathogens and apoptotic cells relies on efficient leukocyte migration into the infectious site, we investigated the regulation of macrophage chemotaxis by miR-466l with C5a, a classic chemoattractant (Gallin and Gallin, 1977), and ATP, a molecule that is released from dying cells as a "find-me signal" (Elliott et al., 2009). Overexpression of miR-466l significantly enhanced human macrophage chemotaxis to both C5a and ATP (Figures 5A and 5B). We did not observe differences in macrophage accumulation in the absence of a chemoattractant. miR-466l also enhanced macrophage chemotaxis to other agonists (Figure S4). Silencing of miR-466l inhibited macrophage chemotaxis to several chemoattractants (Figures 5A and 5B and Figure S4). miR-466l overexpression enhanced macrophage efferocytosis of apoptotic PMNs (Figure 5C), an action inhibited by cytochalasin B (Figure 5D), indicating that miR-466l enhances macrophage chemotaxis and phagocytosis by promoting contractile microfilament formation.

We next questioned whether LMs play a role in mediating phagocytic actions of miR-466l. Incubations of miR-466l-transfected macrophages with a LOX inhibitor (baicalein) led to a reduction in efferocytosis of apoptotic PMNs, whereas RvD1 or a COX inhibitor (indomethacin) significantly increased efferocytosis (Figure 5E), in line with published results (Sadik et al., 2003; Schwab et al., 2007; Yamada and Suzuki, 1989). These findings demonstrate that miR-466l stimulates macrophage efferocytosis in a LOX-dependent manner. Consistent with earlier findings with human PMNs (Levy et al., 2001), exposure of macrophages to COX products PGD_2 and PGE_2 for 18 hr significantly upregulated expression of 15-LOX-1 (Figure 5F), an enzyme involved in SPM production. Amounts of chemotaxis- and phagocytosis-associated proteins, including purinoceptor P_2Y_2 (Elliott et al., 2009), MER tyrosine protein kinase (MERTK) (Scott et al., 2001), and thrombospondin 1 (THBS1) (Savill et al., 1992), were increased by miR-466l overexpression and RvD1 (Figures 5G–5I and Figure S3F). LOX inhibitor downregulated these, an action partially rescued by RvD1 (Figures 5G–5I), suggesting that SPMs act with miR-466l to upregulate chemotaxis- and phagocytosis-associated pathways.

SPMs Regulate miR-466l in Human Leukocytes and Its Identification in Sepsis Patients

With human PMNs and macrophages, Zym dose-dependently increased miR-466l expression (Figure S5A), whereas RvD1, RvD2, and MaR1 (10 nM) each reduced miR-466l (Figures 6A and 6B). In addition, SPMs significantly counterregulated Zym-stimulated miR-466l expression in both cell types, consistent with in vivo findings with murine exudates (Figure 1). Apoptotic PMNs are potent activators of resolution given that macrophage efferocytosis of apoptotic PMNs results in the release of anti-inflammatory cytokines (e.g., TGFβ1 and IL-10) and the biosynthesis of SPMs, including RvE1, PD1, and LXA_4 (Dalli and Serhan, 2012; Freire-de-Lima et al., 2000; Schwab et al., 2007). Similar to RvD1, apoptotic PMNs decreased miR-466l in human primary macrophages (Figures 6C and 6D). These results establish that expression of miR-466l in human primary leukocytes is regulated by proresolving signals, e.g., SPMs and apoptotic PMNs.

We assessed dynamic expression of miR-466l during apoptosis of human PMNs and found that miR-466l was not reduced after 0–12 hr but that it was reduced at 48 hr (>85% of PMNs were apoptotic). Zym delayed PMN apoptosis, whereas serum-treated (opsonized) Zym (STZ) incubation promoted PMN apoptosis (Figure 6E). With Zym, miR-466l accumulated at 4 hr but subsequently reduced at 12 and 48 hr. As expected, STZ reduced miR-466l at 4 and 12 hr yet increased miR-466l at 48 hr (Figure 6E), suggesting that spontaneous apoptotic PMNs and phagocytosis-induced apoptotic PMNs give distinct miR-466l profiles.

In order to assess the potential of miR-466l in disease, we examined the expression of this miRNA in peripheral whole blood and plasma obtained from intensive care unit (ICU) patients with confirmed *Escherichia coli* (*E. coli*) sepsis and from ICU patients without sepsis (control). Samples were collected upon ICU admission, denoted "day 0" (defined as blood collection within 48 hr of ICU admission), and then on days 3 and 7 of the patients' hospital stay. Sepsis patients were divided into those in whom sepsis resolved during hospitalization (sepsis survivors) and those who suffered in-hospital mortality (sepsis nonsurvivors) (Table S4). Real-time PCR results demonstrated that on day 0, miR-466l expression in whole blood of sepsis survivors was significantly higher than that in nonseptic ICU subjects (Figure 6F). miR-466l expression was downregulated in whole-blood samples from sepsis survivors on days 3 and 7. Assessment of plasma miR-466l demonstrated no significant differences between sepsis survivors and nonseptic ICU patients on day 0 (Figure 6F). Also, we found a reduction in plasma miR-466l on both day 3 and day 7 compared to day 0. Compared to both nonseptic ICU patients and sepsis survivors, sepsis nonsurvivors showed a significant increase in both whole-blood and plasma miR-466l on day 0 (Figure 6F). Whole-blood

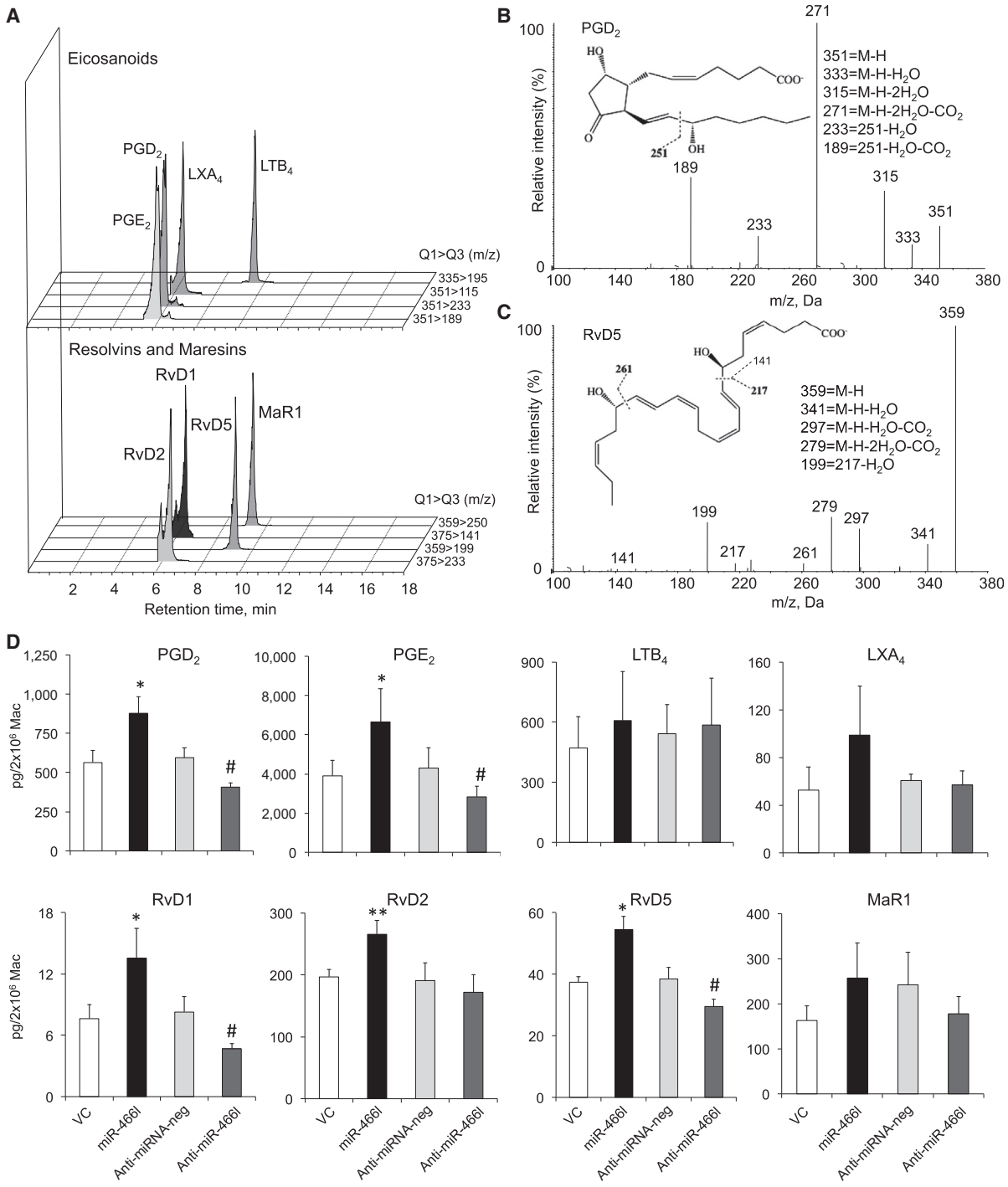

Figure 4. Macrophage LM Profiles Are Regulated by miR-466l

Human macrophages transfected with VC, miR-466l, anti-miRNA-neg, or anti-miR-466l were washed with PBS twice and incubated with Zym (100 ng/ml) for 4 hr. For terminating incubations, ice-cold MeOH was added and samples were subjected to solid-phase extraction. LMs were identified and quantified by LC-MS/MS-based LM metabololipidomics.

(A) Representative multiple-reaction monitoring chromatograms (from three independent experiments) show the elution times for the identified bioactive LMs: Q1, M-H (parent ion); and Q3, diagnostic ion in the tandem mass spectrometry (MS/MS) (daughter ion).

(B) MS/MS spectrum employed for the identification of PGD_2.

(C) MS/MS spectrum employed for the identification of RvD5.

(D) Quantification of arachidonic-acid- and docosahexaenoic-acid-derived LMs was obtained with a calibration curve for each compound. Results are expressed as mean ± SEM from four independent experiments. *$p < 0.05$ and **$p < 0.01$, versus VC; #$p < 0.05$, versus anti-miRNA-neg.

See also Table S3.

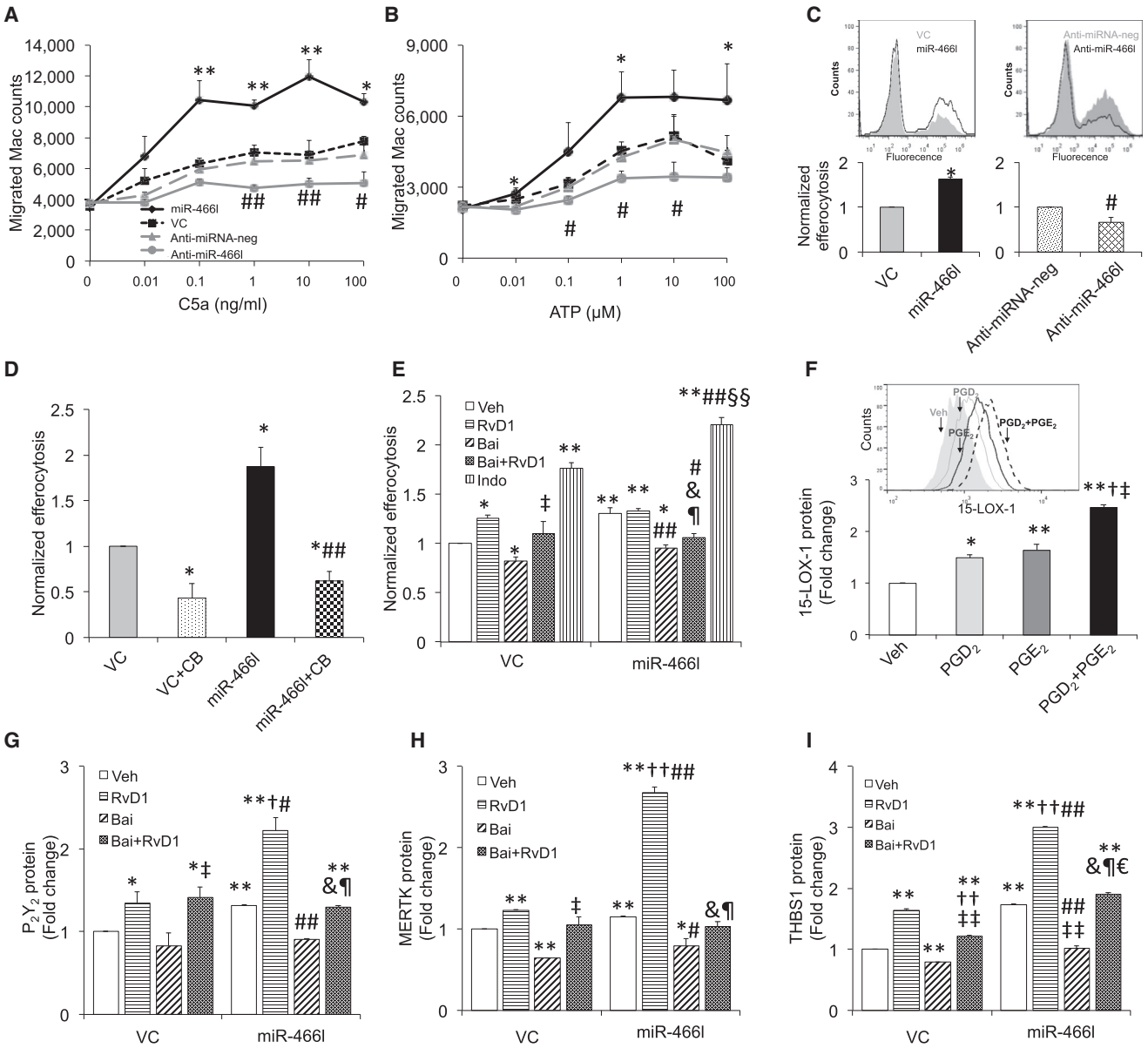

Figure 5. Macrophage Chemotaxis and Efferocytosis Are Enhanced by SPMs and miR-466l

(A–C) Human macrophages were transfected with VC, miR-466l, anti-miRNA-neg, or anti-miR-466l (37°C, 72 hr). Chemotaxis dose response to C5a (A) or ATP (B) is shown. (C) Efferocytosis of apoptotic PMNs (1:3). Results were normalized as fold change of VC or anti-miRNA-neg and expressed as mean ± SEM from at least four independent experiments. *$p < 0.05$ and **$p < 0.01$, versus VC; $^{\#}p < 0.05$ and $^{\#\#}p < 0.01$, versus anti-miRNA-neg.

(D) VC- and miR-466l-transfected human macrophages were treated with cytochalasin B (CB, 1 μg/ml) for 1 hr and incubated with apoptotic PMNs (1:3) for 1 hr. Efferocytosis was assessed with flow cytometry. Results are expressed as mean ± SEM from four independent experiments. *$p < 0.05$ and **$p < 0.01$, versus VC; $^{\#\#}p < 0.01$, versus miR-466l.

(E) VC- and miR-466l-transfected human macrophages were pretreated with PBS (Veh), 10 nM RvD1, 10 μM baicalein (Bai), 10 nM RvD1 plus 10 μM Bai, or 10 μM indomethacin (Indo) for 1 hr and then incubated with apoptotic PMNs (1:3) for 1 hr. Efferocytosis was assessed with flow cytometry. Results are expressed as mean ± SEM from four independent experiments. *$p < 0.05$ and **$p < 0.01$, versus VC Veh; $^{\ddagger}p < 0.05$, versus VC plus Bai; $^{\S\S}p < 0.01$, versus VC plus Indo; $^{\#}p < 0.05$ and $^{\#\#}p < 0.01$, versus miR-466l Veh; $^{\&}p < 0.05$, versus miR-466l plus RvD1; $^{\P}p < 0.05$, versus miR-466l plus Bai.

(F) Human macrophages were incubated with PGD_2 (1 μM), PGE_2 (1 μM), or PGD_2 plus PGE_2 (1 μM each) for 18 hr. Total RNA was isolated, and 15-LOX-1 expression was assessed with flow cytometry. Results are expressed as mean ± SEM from four independent experiments. *$p < 0.05$ and **$p < 0.01$, versus Veh; $^{\dagger}p < 0.05$, versus PGD_2; $^{\ddagger}p < 0.05$, versus PGE_2.

(G–I) VC- and miR-466l-transfected human macrophages were treated with PBS (Veh), 10 nM RvD1, 10 μM Bai, or 10 μM Bai plus 10 nM RvD1 for 18 hr. Expression levels of P_2Y_2 (G), MERTK (H), and THBS1 (I) were assessed with flow cytometry. Results are expressed as mean ± SEM from four independent experiments. *$p < 0.05$ and **$p < 0.01$, versus VC Veh; $^{\dagger\dagger}p < 0.01$, versus VC plus RvD1; $^{\ddagger}p < 0.05$ and $^{\ddagger\ddagger}p < 0.01$, versus VC plus Bai; $^{\in}p < 0.05$, versus VC plus Bai plus RvD1; $^{\#}p < 0.05$ and $^{\#\#}p < 0.01$, versus miR-466l Veh; $^{\&}p < 0.05$, versus miR-466l plus RvD1; $^{\P}p < 0.05$, versus miR-466l plus Bai.

See also Figure S4.

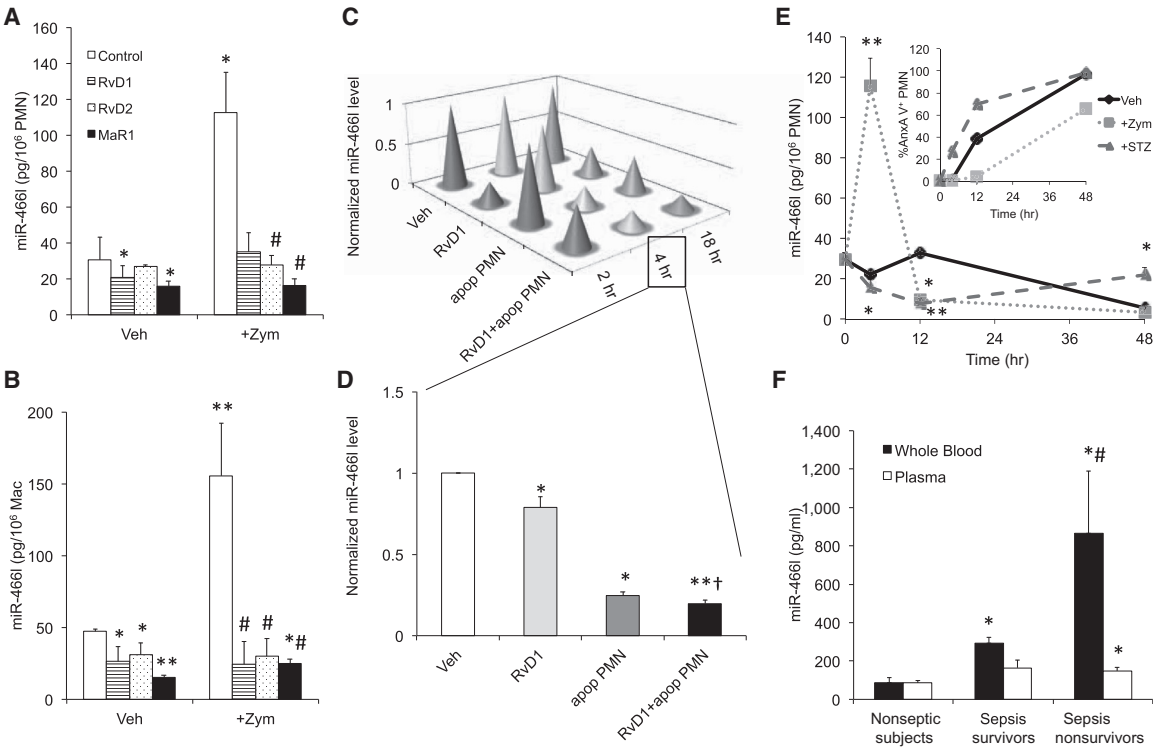

Figure 6. SPMs Regulate miR-466l in Human Leukocytes and Its Identification in Sepsis Patients

(A and B) Human PMNs (10^6 cells/ml) (A) and macrophages (10^6 cells/ml) (B) were incubated with or without Zym (10 ng/ml) (Veh) and 10 nM of SPM (RvD1, RvD2, or MaR1) for 4 hr (PMNs) or 18 hr (macrophages). Expression of miR-466l was assessed by qPCR. Results are expressed as mean ± SEM from five independent experiments. *$p < 0.05$ and **$p < 0.01$, versus Veh control (PBS); #$p < 0.05$, versus Zym alone.

(C) Human macrophages (10^6 cells/ml) were incubated with PBS (Veh), RvD1 (10 nM), and/or apoptotic PMNs (1:3) for 2, 4, and 18 hr, and expression of miR-466l was assessed by qPCR. Results are normalized as fold change of vehicle.

(D) Normalized miR-466l at 4 hr posttreatment is expressed as mean ± SEM from four independent experiments. *$p < 0.05$, versus Veh; †$p < 0.05$, versus RvD1 group.

(E) Human PMNs were incubated with PBS, Zym (10 ng/ml), or STZ (opsonized Zym, 10 ng/ml) for 0–48 hr. Apoptosis (% AnxA V^+ PMNs) was assessed by flow cytometry (top inset, right). miR-466l expression was assessed by qPCR. Results are expressed as mean ± SEM from three independent experiments. *$p < 0.05$ and **$p < 0.01$, versus Veh control (PBS).

(F) Peripheral blood and plasma were collected from nonseptic ICU control patients (nonseptic survivors), *E. coli* sepsis patients who survived, and nonsurvivors of *E. coli* sepsis on day 0 of ICU admission (within 48 hr of ICU admission). See Table S4 for a description of patients. Total RNA was isolated from peripheral blood and plasma, and quantitative miR-466l expression was expressed as mean ± SEM of three patients in each group. *$p < 0.05$, versus nonseptic ICU patients; #$p < 0.05$, versus sepsis patients.

See also Figure S5 and Table S4.

miR-466l amounts in sepsis nonsurvivors on days 3 and 7 were also significantly lower than day 0 values. A similar trend was found with plasma miR-466l on days 3 and 7. Also, we noted that the percentage of miR-466l in plasma was lower in sepsis nonsurvivors than in sepsis survivors and nonseptic ICU subjects on day 0, suggesting that increased miR-466l in sepsis nonsurvivors' blood on day 0 was mostly cell associated.

In these patients, C-reactive protein (CRP), creatinine, IL-1β, IL-6, IL-18, and procalcitonin (PCT) were each increased in sepsis plasma; IL-18 values were statistically significantly higher in the plasma of sepsis nonsurvivors than in the plasma of ICU controls (Table S5 and Figure S5B). This is in line with recent findings that peripheral-blood IL-18 correlates with nonsurvivors of sepsis-induced acute respiratory-distress syndrome (Dolinay et al., 2012). Together, these results indicate that miR-466l is differentially regulated in human peripheral blood during sepsis and that elevation in circulating miR-466l correlates with sepsis nonsurvivors. Hence, in view of our results with murine inflammatory exudates (Figures 1 and 2), these results with sepsis patients suggest that peripheral-blood miR-466l might correlate with an excessive inflammatory phenotype.

AP-1 and NF-κB1 Contribute to SPM-miR-466l Regulatory Networks

Several transcription factors (TFs) are also ARETs, among which are activator protein 1 (AP-1, whose family includes c-Jun and c-Fos) and nuclear factor κB1 (NF-κB1); these ARETs and their phosphorylation were upregulated by miR-466l overexpression (Figures S4A and 7A). We investigated the underlying signaling involved in SPM counterregulation of Zym-stimulated miR-466l. Human macrophages with Zym led to a significant increase in p-JNK, p-p38-AP-1, and IκB-NF-κB1 signals, which were reduced by RvD1, RvD2, and MaR1 (Figures 7B and 7C). Of note, LXA_4 inhibits AP-1 and NF-κB activation in PMNs (József et al., 2002).

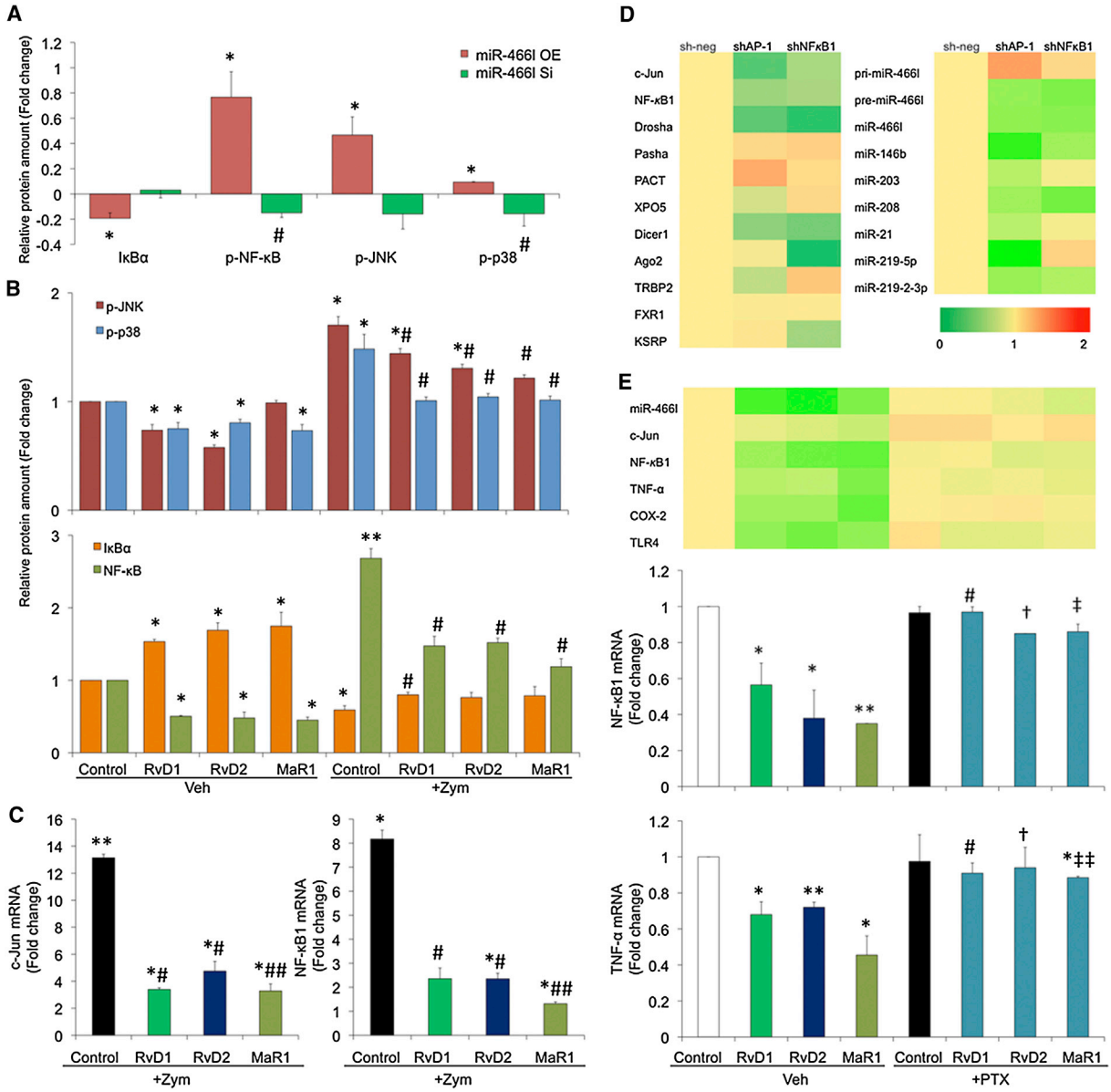

Figure 7. AP-1 and NF-κB1 Contribute to SPM-miR-466l Regulatory Networks

(A) Human macrophages were transfected with VC, miR-466l, anti-miRNA-neg, or anti-miR-466l for 72 hr. Total proteins were isolated for IκBα, p-NF-κB, p-JNK, and p-p38 ELISA (miR-466l overexpression [OE]; miR-466l silencing [Si]). Results are normalized against VC or anti-miRNA-neg and expressed as mean ± SEM from four independent experiments. *$p < 0.05$, versus VC; #$p < 0.05$, versus anti-miRNA-neg.

(B and C) Human macrophages were exposed to Zym (10 ng/ml) and/or SPM (RvD1, RvD2, or MaR1 [10 nM each]) (37°C, 18 hr, pH 7.45). (B) Protein expression of p-JNK, p-p38, IκBα, and NF-κB, and (C) mRNA values of c-Jun and NF-κB1 were assessed with ELISA and qPCR, respectively. Results are expressed as mean ± SEM from five independent experiments. *$p < 0.05$ and **$p < 0.01$, versus Veh control; #$p < 0.05$ and ##$p < 0.01$, versus Zym alone.

(D) Human macrophages were transfected with shAP-1, shNF-κB1, or shscrambled (sh-neg) for 48 hr. Expression levels of miRNA-biogenesis-associated genes, pri-miR-466l, pre-miR-466l, miR-466l, and select resolution-related miRNAs were determined with qPCR. Heatmap results were normalized with sh-neg as controls and are expressed as the mean of five independent experiments.

(E) Human macrophages were preincubated with PTX (100 ng/ml) for 24 hr (37°C, pH 7.45) and then treated with RvD1, RvD2, or MaR1 (10 nM each) for 18 hr (37°C, pH 7.45); expression levels of miR-466l, c-Jun, NF-κB1, TNFα, COX-2, and TLR4 were assessed by qPCR. Heatmap results were normalized against VC and are expressed as the mean of five independent experiments. The results of NF-κB1 and TNFα are expressed as mean ± SEM. *$p < 0.05$ and **$p < 0.01$, versus Veh control; #$p < 0.05$, versus RvD1 Veg; †$p < 0.05$, versus RvD2 Veg; ‡$p < 0.05$ and ‡‡$p < 0.01$, versus MaR1 Veg.

See also Figure S6.

Employing VISTA software (Frazer et al., 2004), we found that the promoters of miRNA-biogenesis-associated genes (Bartel, 2009), including those encoding exportin 5 (XPO5), Dicer1, and transactivation-responsive RNA-binding protein 2 (TRBP2), contain binding sites for AP-1, whereas KSRP (Briata et al., 2011), TRBP2, and argonaute-2 (Ago2) are predicted to be

NF-κB1 targets (Figure S6). In Figure 7D (left panel), a heatmap depicts that AP-1 or NF-κB1 silencing decreased amounts of Drosha and Dicer1. Amounts of both Ago2 and KSRP were also reduced by NF-κB1 RNAi, and AP-1 silencing decreased XPO5 and TRBP2. We next investigated whether inhibition of either AP-1 or NF-κB1 would regulate miR-466l biogenesis and found that inhibition of either in human macrophages led to a significant reduction in precursor miR-466l (pre-miR-466l) and mature miR-466l1 expression, but not in primary miR-466l (pri-miR-466l) expression (Figure 7D, right panel). These results suggest that AP-1 and NF-κB1 promote miR-466l expression in human macrophages by enhancing the maturation process. Inhibition of AP-1 and NF-κB1 also led to downregulation of other resolution-related miRNAs (Recchiuti et al., 2011), including miR-146b, miR-208, and miR-219-2-3p (Figure 7D, right panel). These results demonstrate that AP-1 and NF-κB1 promote the biogenesis of resolution-associated miRNAs.

SPMs activate resolution and display their anti-inflammatory and proresolving actions via G-protein-coupled receptors (GPCRs) (Recchiuti et al., 2011; Serhan, 2007). The amounts of these GPCRs (i.e., LXA_4 receptor [ALX-PR2], RvD1 receptor [DRV1 or GPR32], and RvE1 receptor [ERV1] or chemerin receptor 23 [ChemR23]) were not increased by miR-466l overexpression in human macrophages, but amounts of both DRV1 and ERV1 were decreased by miR-466l silencing (Figure S4A). RvD1, RvD2, and MaR1 actions on miR-466l pathway genes, including those encoding AP-1, NF-κB1, TNFα, COX-2, and TLR4, were blocked by pertussis toxin (PTX) (Figure 7E).

DISCUSSION

Here, we have reported that miR-466l is regulated by Zym and counterregulated by SPMs in human leukocytes and murine inflammatory exudates. Using resolution indices, we first established that (Bannenberg et al., 2005) miR-466l is dynamically regulated during self-limited inflammation in mice and present in peripheral blood of sepsis patients. Overexpression of miR-466l in mice enhanced leukocytic infiltration, regulated exudate leukocyte plasticity, and elevated SPM biosynthesis, thus accelerating clearance of apoptotic PMNs. These findings indicate that miR-466l and SPMs are pivotal in governing the advancement to resolution.

During the resolution phase of the inflammatory response, there is a shift in the leukocyte composition of the inflammatory exudates and a nonphlogistic accumulation of monocytes and macrophages at later time intervals (Serhan and Savill, 2005). In resolving exudates, the main cellular sources of miR-466l are monocytes and macrophages. Hence, miR-466l expression is temporal in that miR-466l is carried with PMN traffic influx to the inflammatory site during initiation and with monocytes and macrophages during resolution, thus dictating the impact of miR-466l in initiation versus programmed resolution. Along these lines, overexpression of miR-466l in murine BMNs increased the amounts of IL-1β, TNF-α, and IL-10, accelerated chemotaxis to C5a and TNFα, and increased ROS production. Injection of miR-466l-transfected BMNs prior to Zym significantly enhanced PMN infiltration at 12 hr. In addition, adoptive transfer of murine peritoneal macrophages overexpressing miR-466l prior to challenge or at the peak of inflammation led to significant reductions in PMN infiltration, shortening the R_i. These results indicate that miR-466l in monocytes and macrophages promotes a proresolving phenotype that facilitates resolution.

Sepsis ICU patients have elevated proinflammatory mediators (Dolinay et al., 2012). The amount of miR-466l in peripheral blood obtained from ICU patients with *E. coli* sepsis was higher in sepsis nonsurvivors than in survivors. We also found with human leukocytes that miR-466l was regulated in a dose-dependent manner after exposure to stimuli. These findings are consistent with the fact that high-dose challenge gave higher amounts of miR-466l in the initiation phase of murine peritonitis than in self-limited inflammation. Thus, together these findings suggest that miR-466l reflects inflammatory status.

LM biosynthesis is temporal during initiation and resolution (Serhan 2007) such that after a self-limited challenge, both leukotrienes and PGs peak during the initiation phase (4–12 hr) and subsequently decline in the resolution phase. In these settings, accumulation of RvD1, RvD2, and RvD5 reached a maximum (amounts known to be bioactive) at the early stage in the resolution phase (Dalli and Serhan, 2012; Fredman et al., 2012). In the present report, miR-466l overexpression promoted RvD1 biosynthesis by upregulating 15-LOX-1 in human macrophages; 15-LOX-1 is a key enzyme for initiating D-series resolvin and protectin production (Dalli and Serhan, 2012). In line with these, miR-466l accumulated early in self-limited inflammation, and its overexpression stimulated an increase in RvD1 in murine inflammatory exudates. Given that in these experimental settings PMNs did not express 12/15-LOX, the murine ortholog of human 15-LOX-1 (Levy et al., 2001), these results suggest that miR-466l expression in macrophages promotes RvD1 biosynthesis, which in turn regulates exudate dissolution. This enhanced biosynthesis of proresolving mediators during the early stages of an inflammatory response is in line with earlier results on the proresolving functions of these mediators, namely stopping further PMN infiltration, stimulating PMN apoptosis (El Kebir et al., 2012) and macrophage efferocytosis, and shortening R_i (Serhan 2007; Serhan and Savill 2005).

In general, miRNAs regulate protein expression by inducing target mRNA degradation or repressing translation. miR-466l was identified in murine embryonic stem cells, macrophages, spleen, and lymph nodes (cf. Calabrese et al., 2007; Chiang et al., 2010) and was found to upregulate IL-10 in murine macrophages (Ma et al., 2010). A hypothesized mechanism via miR-466l antagonizes TTP binding to IL-10 AREs, resulting in reduced IL-10 mRNA decay and relative upregulation (Ma et al., 2010). In the present study, expression profiling of a potential miR-466l target gene indicated that miR-466l upregulated several ARETs, including CD18, IL-10, and TNFα, each of which has complementary UAUUUAU in its 3′ UTR. miR-466l increased 3′ UTR stability of COX-2 and NF-κB1 in macrophages. This is consistent with recent results that specific miRNAs with AREs in the 5′ seed region can switch target mRNA repression to activation by increasing 3′ UTR stability (Mortensen et al., 2011; Vasudevan et al., 2007). Of note, COX-2 is a key enzyme in the production of PGD_2 and PGE_2, mediators that are known to regulate the expression of human 15-LOX-1 and thus promote lipid mediator class switching during the resolution phase of inflammation (Levy et al., 2001). In human macrophages, AP-1 and NF-κB1

promote miR-466l expression by increasing maturation. Because overexpression of miR-466l led to upregulation of resolving macrophage-associated markers, e.g., COX-2, 15-LOX-1, TIMD4, and TGFβ2, and an increase in SPM production, our findings suggest that miR-466l regulates resolution by upregulating SPM biosynthesis, which promotes a homeostatic macrophage phenotype.

SPMs are now appreciated as regulators and markers of M1 and M2 phenotypes (Dalli and Serhan, 2012; Titos et al., 2011) and play roles in both the onset and the resolution of inflammation (Rajakariar et al., 2006; Serhan and Savill, 2005). LM signature profiles have shown that M2 cells produce higher amounts of SPMs, including MaR1, but that they produce lower LTB_4- and COX-derived LMs than do M1 cells (Dalli and Serhan, 2012). Using LC-MS/MS (liquid chromatography-tandem mass spectrometry), we observed the elevation of PGs (e.g., PGD_2 and PGE_2 via COX-2) and SPMs (e.g., RvD1 and RvD5 from 15-LOX) in miR-466l-overexpressing macrophages. These results demonstrate that miR-466l mediates resolution-phase macrophage polarization.

In summation, the present results have established that miR-466l is temporally and differentially expressed during programmed resolution. miR-466l overexpression promotes initiation in PMNs and accelerates resolution in macrophages. In human leukocytes, miR-466l expression is downregulated by resolution signals, including apoptotic PMNs, RvD1, RvD2, and MaR1. Overexpression of miR-466l in macrophages skews populations to a unique resolution-macrophage-like phenotype (Bystrom et al., 2008; Sica and Mantovani, 2012; Stables et al., 2011) that promotes resolution. These populations exhibit enhanced chemotaxis and efferocytosis and upregulated SPM biosynthesis. RvD1 also modulates miR-466l expression as a potential negative feedback during inflammation resolution. In sepsis patients, increased miR-466l correlates with nonsurvival in sepsis. This miR-466l circuit displays pivotal roles in acute inflammatory responses, as demonstrated in peritonitis with regulatory networks involving RNA-binding proteins, TFs, and SPMs. These signaling networks further delineate that resolution actively begins with initiation of inflammation (Serhan and Savill, 2005). Moreover, they provide a molecular basis for delayed resolvers and nonresolving phenotypes in humans (Morris et al., 2010; Pillai et al., 2012). SPM local production and action on leukocyte trafficking and function, as well as miRNA regulation, can exert sustained tissue alterations that permit return to homeostasis.

EXPERIMENTAL PROCEDURES

Chemicals and Reagents

RvD1 (7S,8R,17S-trihydroxy-4Z,9E,11E,13Z,15E,19Z-docosahexaenoic acid), RvD2 (7S,16R,17S-trihydroxy-4Z,8E,10Z,12E,14E,19Z-docosahexaenoic acid; validated according to published criteria, Dalli and Serhan, 2012), PGD_2 (9α,15S-dihydroxy-11-oxo-prosta-5Z,13E-dien-1-oic acid), PGE_2 (9-oxo-11α,15S-dihydroxy-prosta-5Z,13E-dien-1-oic acid), and COX-2 monoclonal FITC antibody were obtained from Cayman Chemical. RvD5 used in these experiments was prepared as in Chiang et al., 2012; MaR1 (7R,14S-dihydrozy-4Z,8E,10E,12Z,16Z,19Z-docosahexaenoic acid; Serhan et al., 2012) was synthesized by Nicos A. Petasis (University of Southern California, P01-GM095467 to C.N.S.). See Supplemental Information for other reagents and chemicals, including real-time PCR primer sequences (Table S5).

miRNA Sequences, Targets, and Gene Nomenclature

The investigated miR-466l has been reported in accordance with the miRBase registry gene annotation and nomenclature (http://www.mirbase.org/) or the National Center for Biotechnology Information (NCBI) database. Targets for miR-466l were obtained with TargetScan (http://www.targetscan.org/), miRDB (http://mirdb.org/miRDB/), and miRanda (http://www.microrna.org/microrna/home.do) with default parameters. The miRBase accession number for mmu-miR-466l-3p is MIMAT0005830.

Murine Peritonitis Model and In Vivo Transfection

Murine peritonitis procedures were approved by the Standing Committee on Animals of Harvard Medical School (protocol 02570) and performed in accordance with institutional guidelines. Murine BMNs and peritoneal macrophage isolation, transfection, and injection are described in the Supplemental Information. Resolution indices were calculated as defined in Schwab et al., 2007 and are as follows: Ψ_{max}, the maximal PMN numbers; T_{max}, the time point of maximal PMN infiltration; Ψ_{50}, 50% of maximal PMNs; T_{50}, the time point when PMN numbers reduced to 50% of the maximum; R_i (resolution interval, T_{50} to T_{max}), the time period when 50% of PMNs were lost from exudates; and K_{50}, the rate of PMN reduction from T_{max} to T_{50}.

Human Subjects

Survivors and nonsurvivors with *E. coli* sepsis were identified from our institutional-review-board-approved Registry of Critical Illness (RoCI) (protocol 2008P000495, Brigham and Women's Hospital [BWH]), in which subjects were enrolled from the BWH ICUs within 48 hr of ICU admission and then characterized as nonseptic ICU controls, sepsis survivors, or sepsis nonsurvivors, as described previously (Dolinay et al., 2012; Nakahira et al., 2011; Sun et al., 2012). Blood was collected upon enrollment ("day 0") and on days 3 and 7 after hospitalization and was stored (–80°C) in PAXgene tubes (QIAGEN). Plasma was isolated and stored (–80°C) from subjects at the same time point. miRNAs were obtained, and miR-466l was measured.

Preparation of Apoptotic PMNs, Leukocyte Functions, and LC-MS/MS-Based Targeted LM Metabololipidomics

PMNs were isolated from fresh peripheral blood of healthy volunteers as described (protocol 1999-P-001297, approved by the Partners Human Research Committee, Boston). Fluorescently labeled apoptotic human PMNs were obtained after overnight incubation in RPMI 1640 of freshly isolated PMNs prelabeled with CFDA (10 μM; Sigma). Human macrophage isolation, transfections, leukocyte functional assays (ROS, chemotaxis, efferocytosis), and luciferase assays, as well as metabololipidomics, are described in the Supplemental Information.

Statistical Analysis

All results are expressed as mean ± SEM. Statistical differences between groups were compared with a Student's t test or one-way ANOVA. $p < 0.05$ was considered statistically significant.

ACCESSION NUMBERS

The microarray data are available in the Gene Expression Omnibus (GEO) database (http://www.ncbi.nlm.nih.gov/gds) under the accession number GSE52174.

SUPPLEMENTAL INFORMATION

Supplemental Information includes Supplemental Experimental Procedures, seven figures, and six tables and can be found with this article online at http://dx.doi.org/10.1016/j.immuni.2013.10.011.

ACKNOWLEDGMENTS

We thank Gabrielle Fredman for providing some of the murine exudates. We appreciate Mary H. Small for expert help in manuscript preparation. This work was supported by National Institutes of Health grants R01-GM038765 (C.N.S.) and R01-HL112747 (R.M.B.). The authors are grateful to the members

of the BWH Registry of Critical Illness (A.M. Choi, A.F. Massaro, L.E. Fredenburgh, L. Gazourian, J.A. Englert, A. Rogers, and T. Dolinay) for their help with human subjects studies, and special thanks go to Anna Trtchounian for assistance with preparing the manuscript. C.N.S. is an inventor of patents (resolvins) assigned to BWH and licensed to Resolvyx Pharmaceuticals. C.N.S. was scientific founder of Resolvyx Pharmaceuticals and owns founder stock in the company. C.N.S.'s interests were reviewed and are managed by BWH and Partners HealthCare in accordance with their conflict-of-interest policies.

Received: November 15, 2012
Accepted: October 25, 2013
Published: November 14, 2013

REFERENCES

Asirvatham, A.J., Magner, W.J., and Tomasi, T.B. (2009). miRNA regulation of cytokine genes. Cytokine *45*, 58–69.

Bannenberg, G.L., Chiang, N., Ariel, A., Arita, M., Tjonahen, E., Gotlinger, K.H., Hong, S., and Serhan, C.N. (2005). Molecular circuits of resolution: formation and actions of resolvins and protectins. J. Immunol. *174*, 4345–4355.

Bartel, D.P. (2009). MicroRNAs: target recognition and regulatory functions. Cell *136*, 215–233.

Briata, P., Chen, C.Y., Giovarelli, M., Pasero, M., Trabucchi, M., Ramos, A., and Gherzi, R. (2011). KSRP, many functions for a single protein. Front Biosci (Landmark Ed) *16*, 1787–1796.

Bystrom, J., Evans, I., Newson, J., Stables, M., Toor, I., van Rooijen, N., Crawford, M., Colville-Nash, P., Farrow, S., and Gilroy, D.W. (2008). Resolution-phase macrophages possess a unique inflammatory phenotype that is controlled by cAMP. Blood *112*, 4117–4127.

Calabrese, J.M., Seila, A.C., Yeo, G.W., and Sharp, P.A. (2007). RNA sequence analysis defines Dicer's role in mouse embryonic stem cells. Proc. Natl. Acad. Sci. USA *104*, 18097–18102.

Chiang, H.R., Schoenfeld, L.W., Ruby, J.G., Auyeung, V.C., Spies, N., Baek, D., Johnston, W.K., Russ, C., Luo, S., Babiarz, J.E., et al. (2010). Mammalian microRNAs: experimental evaluation of novel and previously annotated genes. Genes Dev. *24*, 992–1009.

Chiang, N., Fredman, G., Bäckhed, F., Oh, S.F., Vickery, T., Schmidt, B.A., and Serhan, C.N. (2012). Infection regulates pro-resolving mediators that lower antibiotic requirements. Nature *484*, 524–528.

Dalli, J., and Serhan, C.N. (2012). Specific lipid mediator signatures of human phagocytes: microparticles stimulate macrophage efferocytosis and pro-resolving mediators. Blood *120*, e60–e72.

Dolinay, T., Kim, Y.S., Howrylak, J., Hunninghake, G.M., An, C.H., Fredenburgh, L., Massaro, A.F., Rogers, A., Gazourian, L., Nakahira, K., et al. (2012). Inflammasome-regulated cytokines are critical mediators of acute lung injury. Am. J. Respir. Crit. Care Med. *185*, 1225–1234.

El Kebir, D., Gjorstrup, P., and Filep, J.G. (2012). Resolvin E1 promotes phagocytosis-induced neutrophil apoptosis and accelerates resolution of pulmonary inflammation. Proc. Natl. Acad. Sci. USA *109*, 14983–14988.

Elliott, M.R., Chekeni, F.B., Trampont, P.C., Lazarowski, E.R., Kadl, A., Walk, S.F., Park, D., Woodson, R.I., Ostankovich, M., Sharma, P., et al. (2009). Nucleotides released by apoptotic cells act as a find-me signal to promote phagocytic clearance. Nature *461*, 282–286.

Frazer, K.A., Pachter, L., Poliakov, A., Rubin, E.M., and Dubchak, I. (2004). VISTA: computational tools for comparative genomics. Nucleic Acids Res. *32* (Web Server issue), W273–W279.

Fredman, G., Li, Y., Dalli, J., Chiang, N., and Serhan, C.N. (2012). Self-limited versus delayed resolution of acute inflammation: temporal regulation of pro-resolving mediators and microRNA. Sci Rep *2*, 639.

Freire-de-Lima, C.G., Nascimento, D.O., Soares, M.B., Bozza, P.T., Castro-Faria-Neto, H.C., de Mello, F.G., DosReis, G.A., and Lopes, M.F. (2000). Uptake of apoptotic cells drives the growth of a pathogenic trypanosome in macrophages. Nature *403*, 199–203.

Gallin, E.K., and Gallin, J.I. (1977). Interaction of chemotactic factors with human macrophages. Induction of transmembrane potential changes. J. Cell Biol. *75*, 277–289.

Gordon, S. (2007). The macrophage: past, present and future. Eur. J. Immunol. *37* (*Suppl 1*), S9–S17.

József, L., Zouki, C., Petasis, N.A., Serhan, C.N., and Filep, J.G. (2002). Lipoxin A4 and aspirin-triggered 15-epi-lipoxin A4 inhibit peroxynitrite formation, NF-kappa B and AP-1 activation, and IL-8 gene expression in human leukocytes. Proc. Natl. Acad. Sci. USA *99*, 13266–13271.

Kyritsis, N., Kizil, C., Zocher, S., Kroehne, V., Kaslin, J., Freudenreich, D., Iltzsche, A., and Brand, M. (2012). Acute inflammation initiates the regenerative response in the adult zebrafish brain. Science *338*, 1353–1356.

Levy, B.D., Clish, C.B., Schmidt, B., Gronert, K., and Serhan, C.N. (2001). Lipid mediator class switching during acute inflammation: signals in resolution. Nat. Immunol. *2*, 612–619.

Ma, F., Liu, X., Li, D., Wang, P., Li, N., Lu, L., and Cao, X. (2010). MicroRNA-466l upregulates IL-10 expression in TLR-triggered macrophages by antagonizing RNA-binding protein tristetraprolin-mediated IL-10 mRNA degradation. J. Immunol. *184*, 6053–6059.

McCusker, J.H., Clemons, K.V., Stevens, D.A., and Davis, R.W. (1994). Genetic characterization of pathogenic Saccharomyces cerevisiae isolates. Genetics *136*, 1261–1269.

Mitchell, P.S., Parkin, R.K., Kroh, E.M., Fritz, B.R., Wyman, S.K., Pogosova-Agadjanyan, E.L., Peterson, A., Noteboom, J., O'Briant, K.C., Allen, A., et al. (2008). Circulating microRNAs as stable blood-based markers for cancer detection. Proc. Natl. Acad. Sci. USA *105*, 10513–10518.

Morris, T., Stables, M., Colville-Nash, P., Newson, J., Bellingan, G., de Souza, P.M., and Gilroy, D.W. (2010). Dichotomy in duration and severity of acute inflammatory responses in humans arising from differentially expressed proresolution pathways. Proc. Natl. Acad. Sci. USA *107*, 8842–8847.

Mortensen, R.D., Serra, M., Steitz, J.A., and Vasudevan, S. (2011). Posttranscriptional activation of gene expression in Xenopus laevis oocytes by microRNA-protein complexes (microRNPs). Proc. Natl. Acad. Sci. USA *108*, 8281–8286.

Nakahira, K., Haspel, J.A., Rathinam, V.A., Lee, S.J., Dolinay, T., Lam, H.C., Englert, J.A., Rabinovitch, M., Cernadas, M., Kim, H.P., et al. (2011). Autophagy proteins regulate innate immune responses by inhibiting the release of mitochondrial DNA mediated by the NALP3 inflammasome. Nat. Immunol. *12*, 222–230.

Pillai, P.S., Leeson, S., Porter, T.F., Owens, C.D., Kim, J.M., Conte, M.S., Serhan, C.N., and Gelman, S. (2012). Chemical mediators of inflammation and resolution in post-operative abdominal aortic aneurysm patients. Inflammation *35*, 98–113.

Rajakariar, R., Yaqoob, M.M., and Gilroy, D.W. (2006). COX-2 in inflammation and resolution. Mol. Interv. *6*, 199–207.

Recchiuti, A., Krishnamoorthy, S., Fredman, G., Chiang, N., and Serhan, C.N. (2011). MicroRNAs in resolution of acute inflammation: identification of novel resolvin D1-miRNA circuits. FASEB J. *25*, 544–560.

Russell, D.G., and Gordon, S. (2009). Phagocyte-pathogen interactions: macrophages and the host response to infection. (Washington, DC: ASM Press).

Sadik, C.D., Sies, H., and Schewe, T. (2003). Inhibition of 15-lipoxygenases by flavonoids: structure-activity relations and mode of action. Biochem. Pharmacol. *65*, 773–781.

Savill, J., Hogg, N., Ren, Y., and Haslett, C. (1992). Thrombospondin cooperates with CD36 and the vitronectin receptor in macrophage recognition of neutrophils undergoing apoptosis. J. Clin. Invest. *90*, 1513–1522.

Schif-Zuck, S., Gross, N., Assi, S., Rostoker, R., Serhan, C.N., and Ariel, A. (2011). Saturated-efferocytosis generates pro-resolving CD11b low macrophages: modulation by resolvins and glucocorticoids. Eur. J. Immunol. *41*, 366–379.

Schwab, J.M., Chiang, N., Arita, M., and Serhan, C.N. (2007). Resolvin E1 and protectin D1 activate inflammation-resolution programmes. Nature *447*, 869–874.

Scott, R.S., McMahon, E.J., Pop, S.M., Reap, E.A., Caricchio, R., Cohen, P.L., Earp, H.S., and Matsushima, G.K. (2001). Phagocytosis and clearance of apoptotic cells is mediated by MER. Nature *411*, 207–211.

Serhan, C.N. (2007). Resolution phase of inflammation: novel endogenous anti-inflammatory and proresolving lipid mediators and pathways. Annu. Rev. Immunol. *25*, 101–137.

Serhan, C.N., and Savill, J. (2005). Resolution of inflammation: the beginning programs the end. Nat. Immunol. *6*, 1191–1197.

Serhan, C.N., Dalli, J., Karamnov, S., Choi, A., Park, C.K., Xu, Z.Z., Ji, R.R., Zhu, M., and Petasis, N.A. (2012). Macrophage proresolving mediator maresin 1 stimulates tissue regeneration and controls pain. FASEB J. *26*, 1755–1765.

Sica, A., and Mantovani, A. (2012). Macrophage plasticity and polarization: in vivo veritas. J. Clin. Invest. *122*, 787–795.

Sonkoly, E., and Pivarcsi, A. (2009). microRNAs in inflammation. Int. Rev. Immunol. *28*, 535–561.

Stables, M.J., Shah, S., Camon, E.B., Lovering, R.C., Newson, J., Bystrom, J., Farrow, S., and Gilroy, D.W. (2011). Transcriptomic analyses of murine resolution-phase macrophages. Blood *118*, e192–e208.

Sun, X., Icli, B., Wara, A.K., Belkin, N., He, S., Kobzik, L., Hunninghake, G.M., Vera, M.P., Blackwell, T.S., Baron, R.M., and Feinberg, M.W.; MICU Registry. (2012). MicroRNA-181b regulates NF-κB-mediated vascular inflammation. J. Clin. Invest. *122*, 1973–1990.

Titos, E., Rius, B., González-Périz, A., López-Vicario, C., Morán-Salvador, E., Martínez-Clemente, M., Arroyo, V., and Clària, J. (2011). Resolvin D1 and its precursor docosahexaenoic acid promote resolution of adipose tissue inflammation by eliciting macrophage polarization toward an M2-like phenotype. J. Immunol. *187*, 5408–5418.

Underhill, D.M., Ozinsky, A., Hajjar, A.M., Stevens, A., Wilson, C.B., Bassetti, M., and Aderem, A. (1999). The Toll-like receptor 2 is recruited to macrophage phagosomes and discriminates between pathogens. Nature *401*, 811–815.

Vasudevan, S., and Steitz, J.A. (2007). AU-rich-element-mediated upregulation of translation by FXR1 and Argonaute 2. Cell *128*, 1105–1118.

Vasudevan, S., Tong, Y., and Steitz, J.A. (2007). Switching from repression to activation: microRNAs can up-regulate translation. Science *318*, 1931–1934.

Yamada, A., and Suzuki, T. (1989). Fc gamma 2b receptor-mediated phagocytosis by a murine macrophage-like cell line (P388D1) and peritoneal resident macrophages. Up-regulation by the inhibitors of phospholipase A2 and cyclooxygenase. J. Immunol. *142*, 2457–2463.